



HAL
open science

A nonlinear model for combustion instability: analysis and quenching of the oscillations

Ioan Doré Landau, Fethi Bouziani, Robert Bitmead

► **To cite this version:**

Ioan Doré Landau, Fethi Bouziani, Robert Bitmead. A nonlinear model for combustion instability: analysis and quenching of the oscillations. A. Astolfi, L. Marconi. Analysis and design of nonlinear control systems, Springer, pp.100-119, 2007. hal-00133806

HAL Id: hal-00133806

<https://hal.science/hal-00133806>

Submitted on 27 Feb 2007

HAL is a multi-disciplinary open access archive for the deposit and dissemination of scientific research documents, whether they are published or not. The documents may come from teaching and research institutions in France or abroad, or from public or private research centers.

L'archive ouverte pluridisciplinaire **HAL**, est destinée au dépôt et à la diffusion de documents scientifiques de niveau recherche, publiés ou non, émanant des établissements d'enseignement et de recherche français ou étrangers, des laboratoires publics ou privés.

A non linear model for combustion instability : analysis and quenching of the oscillations

Ioan D. Landau¹, Fethi Bouziani,² and Robert R. Bitmead³

¹ Laboratoire d'Automatique de Grenoble, ENSIEG BP 46, 38402 Saint-Martin d'Hères, France landau@lag.ensieg.inpg.fr

² Laboratoire d'Automatique de Grenoble, ENSIEG BP 46, 38402 Saint-Martin d'Hères, France Fethi.Bouziani@lag.ensieg.inpg.fr

³ Department of Mechanical & Aerospace Engineering, University of California, San Diego, La Jolla CA 92093-0411, USA rbitmead@ucsd.edu

Prelude

It is a great pleasure for us to contribute to this book dedicated to Alberto Isidori on the occasion of his sixty fifth birthday. It is also, for the first author, the occasion to acknowledge a very long period of useful and pleasant exchange which started in 1973 (bilinear systems) and has continued through the years on various specific subjects.

The important contributions of Alberto Isidori in the control of nonlinear systems have had a tremendous impact in the control community. Feedback linearization was one of the important subjects developed by Alberto. While the oscillatory nonlinear system considered in this contribution requires specific techniques for its analysis, still a feedback linearization is used for quenching the oscillations.

1 Introduction

Combustion instabilities phenomena in gas turbine are the focus of several investigations started from more than 200 years [1]. Recent important research programs oriented on this topic are conducted in some countries with industrial collaboration (*inter alia* USA, France and UK). The papers [2, 3, 4, 5] give an overview of this activity. These phenomena are extremely complex and hard to predict, but in most cases it can be explained by an unsteady flame generating pressure waves which are reflected by physical boundaries into the combustion process. In term of system interpretation, this correspond to a positive feedback coupling between the heat-release process and acoustics of the combustion chamber (Figure 1). The positive feedback coupling leads to the creation of nonlinear limit cycles. Generally, these phenomena occur only

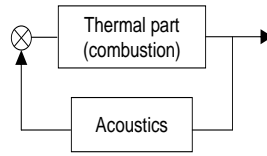


Fig. 1. Positive feedback coupling between the heat-release process and acoustics.

in the confined environments. The Rijke tube [6] which consists of flame placed inside an open-ended cylinder (Figure 2), is one simple demonstration that shows that instabilities occur in the confined environments.

The heart of the issue is that combustion at low equivalence ratio (fuel-to-air ratio) is desirable for reducing pollution. Unfortunately, as equivalence ratio decreases the instability appears and manifests itself through strong self-sustained oscillations, which can be sometimes characterized by the coexistence of oscillations at several distinct non-harmonic frequencies.

From a practical perspective, the modulation of a fuel flow fraction into the combustor is possible as a control input (of multiplicative type). This modulation has been widely tested in experiments as a candidate for active control for suppressing the combustion instability [7, 8]. In the literature, several active control methods have been proposed; an excellent overview of existing methods is given in [5]. Systematic design and implementation of active control requires a realistic low order model which exhibits the dominant dynamical effects. The parsimonious modelling of such nonlinear systems is an extremely difficult task, given that high-order, physics-based computational fluid dynamical codes can be unreliable in demonstrating the phenomenon well. One particular feature which the model should capture is the simultaneous coexistence of two non-harmonic oscillating modes [9, 10].

Establishing a low order model requires a good knowledge of the physical phenomenon in same time the availability of mathematical tools allowing the analysis of nonlinear oscillating systems. The models presented in the literature are established according to various approaches. Some models are established by a purely theoretical approach starting from physical equations of combustion process while others by a purely experimental approach. However, there exist models which are established on a compromise between the theoretical approach and the experimental approach (gray-box approach). Among these models, Dunstan and Bitmead model [11] represents good base for understanding the instabilities mechanism. Unfortunately, in the absence of analysis tools this model loses much of its utility. This leads that for such system, the first step of model identification can be seen as the association between the powerful analysis methods and existing models. The Krylov-Bogoliubov (K-B) method (detailed in [12, 13, 14, 15, 16]) is one of analysis methods widely used for nonlinear oscillating systems. From our knowledge, this work is the first application of K-B method for analysis of combustion instabilities models. The effectiveness of this method combined

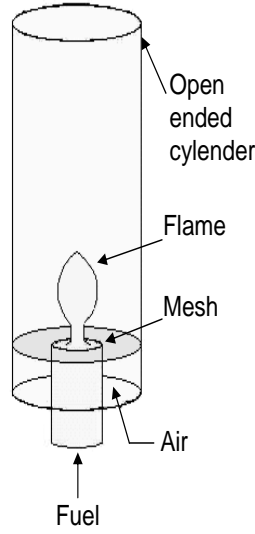


Fig. 2. Rijke tube.

with a relevant model may be considered as the solution of combustion instabilities modelling problem.

The model presented in this chapter, inspired from [11], is an analytically tractable model for combustion instabilities. The chapter is organized as follows. In Section 2, a summarize of the first K-B approximation for autonomous multi-resonator systems is present. To illustrate efficiency of K-B approximation and multiplicative control, in Section 3, a generalized Van der Pol equation is considered as a reduced-order model for combustion instabilities. In Section 4, a multiple-resonator model is presented and analyzed using K-B method. This model is employed in Section 5 for studying the possibility of quenching of the oscillations in combustion instabilities by multiplicative control. In Section 6, conclusion and further work remarks are given.

2 First K-B approximation for autonomous multi-resonator systems

Consider a system with n resonators described by differential equations of the form,

$$\frac{d^2x_j}{dt^2} + \omega_j^2 x_j = \epsilon f_j \left(x, \frac{dx}{dt} \right), \quad (j = 1, 2, \dots, n), \quad (1)$$

where $x = \{x_1, \dots, x_n\}$, $\frac{dx}{dt} = \{\frac{dx_1}{dt}, \dots, \frac{dx_n}{dt}\}$ and ϵ is a small parameter. For the j th resonator, the first K-B approximation (for more details see Chapter 2 of [15]) proposes the solution

$$x_j = a_j \cos(\psi_j), \quad (2)$$

where $\psi_j = \omega_j t + \theta_j$, a_j and θ_j are slowly time-varying functions obeying the equations

$$\begin{cases} \frac{da_j}{dt} = -\frac{\epsilon}{2\omega_j} H_{jj}(a_1, \dots, a_n, \theta_1, \dots, \theta_n), \\ \frac{d\theta_j}{dt} = -\frac{\epsilon}{2\omega_j a_j} G_{jj}(a_1, \dots, a_n, \theta_1, \dots, \theta_n), \end{cases} \quad (3)$$

with H_{jj} and G_{jj} obtained from the function $f_j(x, \frac{dx}{dt})$ by substituting

$$\begin{cases} x_k = a_k \cos(\omega_k t + \theta_k), \\ \frac{dx_k}{dt} = -a_k \omega_k \sin(\omega_k t + \theta_k), \end{cases} \quad (k = 1, 2, \dots, n) \quad (4)$$

and by setting it in the form

$$\begin{aligned} f_j(a_1 \cos(\omega_1 t + \theta_1), \dots, a_n \cos(\omega_n t + \theta_n), -a_1 \omega_1 \sin(\omega_1 t + \theta_1), \dots, \\ -a_n \omega_n \sin(\omega_n t + \theta_n)) = H_{jj} \sin(\omega_j t + \theta_j) + G_{jj} \cos(\omega_j t + \theta_j) \\ + \sum_{\substack{r \\ \omega_j \neq \omega_\ell}} (H_{\ell j} \sin(\omega_\ell t + \theta_\ell) + G_{\ell j} \cos(\omega_\ell t + \theta_\ell)), \end{aligned} \quad (5)$$

where ω_ℓ and θ_ℓ are integer linear combinations of $\omega_1, \dots, \omega_n$ and $\theta_1, \dots, \theta_n$, respectively, and r is the number of possible integer linear combinations of $\omega_1, \dots, \omega_n$ different from ω_j . For x_j the coefficients of the fundamental term in (5) are used and the all other terms are eliminated.

3 Simple case study: generalized Van der Pol equation

In this section a reduced-order model for combustion instabilities with one single resonator (corresponding to a generalized Van der Pol equation) will be considered to illustrate the potential effectiveness of K-B method for analysis and the closed-loop multiplicative control for quenching the oscillations.

3.1 Model analysis

Consider the Van der Pol equation in generalized form (Figure 3).

$$\ddot{x} + \omega^2 x = \frac{d}{dt} \left\{ \varphi_{v0} + \varphi_{v1} x - \frac{\varphi_{v3}}{3} x^3 \right\}, \quad (6)$$

where ω is the natural frequency, φ_{v1} and φ_{v3} are arbitrary positive constants, φ_{v0} is an arbitrary constant, $p = x$ is the downstream pressure perturbation at the burning plane, and $q = \varphi_{v0} + \varphi_{v1} x - \frac{\varphi_{v3}}{3} x^3$ is the flame heat release rate.

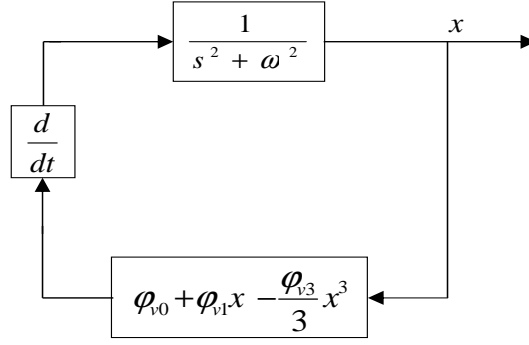


Fig. 3. A simplified combustion instabilities model.

Lemma 1. For the Van der Pol equation (6), the application of K-B approximation gives

$$x = a \cos(\omega t + \theta) \quad (7)$$

with

$$\begin{cases} \dot{a} = \frac{\varphi_{v1}}{2} a \left(1 - \frac{\varphi_{v3}}{4\varphi_{v1}} a^2 \right) \\ \dot{\theta} = 0 \end{cases} \quad (8)$$

Proof: consider the equation (6) and the form (1), in this case ($\epsilon = 1$)

$$f(x, \frac{dx}{dt}) = \varphi_{v1} \left(1 - \frac{\varphi_{v3}}{\varphi_{v1}} x^2 \right) \frac{dx}{dt}. \quad (9)$$

Introducing $x = a \cos(\omega t + \theta)$ and $\dot{x} = -a\omega \sin(\omega t + \theta)$, $i = 1, 2$, in (9), one gets

$$f(.,.) = -\omega\varphi_{v1}a \left(1 - \frac{\varphi_{v3}}{4\varphi_{v1}} a^2 \right) \sin(\omega t + \theta) - \frac{\omega\varphi_{v3}a^3}{4} \sin(3(\omega t + \theta)). \quad (10)$$

Consequently, one can consider that (10) is in the form (5). Thus for x one obtains

$$\begin{cases} H_1 = -\omega\varphi_{v1}a \left(1 - \frac{\varphi_{v3}}{4\varphi_{v1}} a^2 \right) \\ G_1 = 0 \end{cases} \quad (11)$$

By the application of rule (3) on (11), one deduces the result on lemma 1.

The equations system (8) have two steady-state solutions. One steady-state solution corresponds to $a = 0$, and it is unstable. The other steady-state solution correspond to $a = 2\sqrt{\frac{\varphi_{v1}}{\varphi_{v3}}}$, and it is locally stable. Therefore, we conclude for the uncontrolled generalized van der Pol equation, that the solution x is a self-sustained oscillation with steady frequency close to ω and with steady state amplitude close to $2\sqrt{\frac{\varphi_{v1}}{\varphi_{v3}}}$.

3.2 Quenching of the oscillations

The output-feedback control is introduced into the model by multiplying a function of the output x to capture the effect of fuel flow modulation on the heat release rate. The control strategy is characterized by the following differential equation.

$$\ddot{x} + \omega^2 x = \frac{d}{dt} \left\{ (1 + \Phi(x)) \left(\varphi_{v0} + \varphi_{v1}x - \frac{\varphi_{v3}}{3}x^3 \right) \right\}, \quad (12)$$

where φ_{v0} is different from zero and the feedback law $\Phi(x)$ is a polynomial function of x . In order to quench self-sustained oscillation, the control law must force the system (12) to be asymptotically stable at the origin. Hence, one considers the following lemma.

Lemma 2. *For the following control law*

$$\Phi(x) = -Kx - \frac{1}{\varphi_{v0}} \left(\varphi_{v1}x - \frac{\varphi_{v3}}{3}x^3 \right), \quad (13)$$

where K is a constant of the same sign of φ_{v0} , the system (12) is locally asymptotically stable at the origin.

Proof: Introducing the expression (13) into the differential equation (12), one gets

$$\ddot{x} + \omega^2 x = -K\varphi_{v0}\dot{x} - 2\varphi_{v1} \left(K + \frac{\varphi_{v1}}{\varphi_{v0}} \right) x\dot{x} + \frac{4\varphi_{v3}}{3} \left(K + \frac{2\varphi_{v1}}{\varphi_{v0}} \right) x^3\dot{x} - 2\frac{\varphi_{v3}^2}{3\varphi_{v0}} x^5\dot{x}$$

Expressing this equation in state equation form with $z_1 = x$ and $z_2 = \dot{x}$, one obtains

$$\begin{cases} \dot{z}_1 = z_2 \\ \dot{z}_2 = -\omega^2 z_1 - K\varphi_{v0}z_2 - 2\varphi_{v1} \left(K + \frac{\varphi_{v1}}{\varphi_{v0}} \right) z_1 z_2 \\ \quad + \frac{4\varphi_{v3}}{3} \left(K + \frac{2\varphi_{v1}}{\varphi_{v0}} \right) z_1^3 z_2 - 2\frac{\varphi_{v3}^2}{3\varphi_{v0}} z_1^5 z_2 \end{cases} .$$

Computation of the linearized system matrix around the origin gives

$$A_z = \begin{bmatrix} 0 & 1 \\ -\omega^2 & -K\varphi_{v0} \end{bmatrix}, \quad (14)$$

since by assumption K and φ_{v0} have the same sign, the eigenvalues of matrix A_z will have negative real part. By using Lyapunov's indirect method, one can deduce that the system is locally asymptotically stable at the origin.

The local asymptotical stability at the origin implies that quenching of the oscillation is possible and can occur in a local domain around the origin which can be estimated [17]. This quenching is illustrated by the simulation test presented in Figure 4.

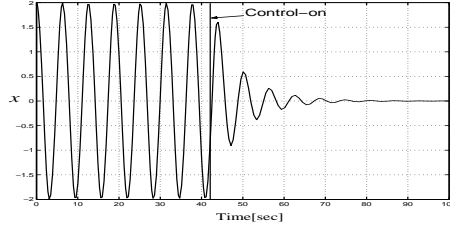


Fig. 4. Simulation test of quenching oscillations on a model described by a generalized van der Pol equation, where $K = 1$, $\varphi_{v0} = 0.45$, $\varphi_{v1} = \varphi_{v1} = 0.1$ and $\omega = 1$.

4 Combustion instability model

The relationship between coupled Van der Pol equations and combustion instabilities model of Dunstan and Bitmead [11] has been discussed in [18]. A system of two coupled Van der Pol equations has been considered as a basic model for combustion instabilities

$$\begin{cases} \frac{d^2 x_1}{dt^2} + \omega_1^2 x_1 = \epsilon \frac{d}{dt} \left((x_1 + x_2) - \frac{1}{3} (x_1 + x_2)^3 \right), \\ \frac{d^2 x_2}{dt^2} + \omega_2^2 x_2 = \epsilon \frac{d}{dt} \left((x_1 + x_2) - \frac{1}{3} (x_1 + x_2)^3 \right), \end{cases} \quad (15)$$

where ω_1 and ω_2 are the natural radian frequencies of the first and second resonators respectively and which can have arbitrary values with some modest provisions to be developed, ϵ is a small positive quantity. The model has been successfully analyzed using Krylov-Bogoliubov approach in [18]. However, this model does not include the cascade differentiator - delay and the low pass filter (existing in Dunstan and Bitmead model [11]). While interesting results have been obtained concerning the existence or quenching of the oscillations in the system, the model was not able to explain the simultaneous presence of two oscillating non-harmonic modes observed experimentally.

In order to make modelling more realistic in [19], the model based on two coupled Van der Pol equations was further generalized by incorporating delay and filtering. The modifications lead to the model presented in Figure 5 and is described by the following equations

$$\begin{cases} \ddot{x}_1 + \omega_1^2 x_1 = \frac{d}{dt} LPF \left\{ \varphi_{v0} + \varphi_{v1} \dot{p}_\tau - \frac{\varphi_{v3}}{3} \dot{p}_\tau^3 \right\}, \\ \ddot{x}_2 + \omega_2^2 x_2 = \frac{d}{dt} LPF \left\{ \varphi_{v0} + \varphi_{v1} \dot{p}_\tau - \frac{\varphi_{v3}}{3} \dot{p}_\tau^3 \right\}, \end{cases} \quad (16)$$

where φ_{v0} is an arbitrary constant, φ_{v1} and φ_{v3} are arbitrary negative constants, τ is a transport time delay from nozzle to flame surface, LPF is the transfer operator of the low pass filter, $p = x_1 + x_2$ is the downstream pressure perturbation at the burning plane, \dot{p}_τ is the output of the delay-plus-differentiator block and q is the flame heat release rate.

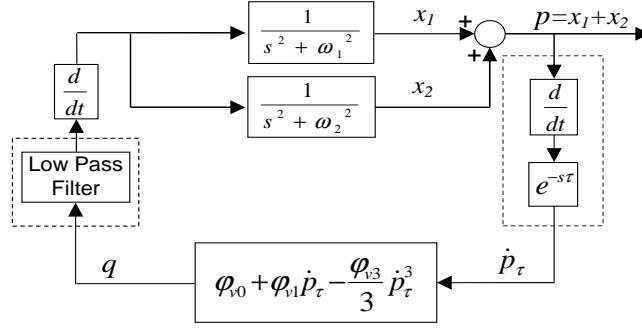


Fig. 5. Proposed combustion instability model.

4.1 Model analysis

Equation development and analysis

The first step of analysis is to develop the left term of equations (16) in order to apply K-B approximation. The presence of delay and low pass filtering yields some difficulties in computing approximations, which will be treated by introducing some realistic assumptions which are effective in stationary regime. Consider the system (16) and the form (1) (with $\epsilon = 1$), in this case

$$f_1 = f_2 = f = \frac{d}{dt} LPF \left\{ \varphi_{v0} + \varphi_{v1} \dot{p}_\tau - \frac{\varphi_{v3}}{3} \dot{p}_\tau^3 \right\}. \quad (17)$$

Replacing

$$\dot{x}_i = -a_i \omega_i \sin(\omega_i t + \theta_i), (i = 1, 2)$$

in \dot{p} , one obtains

$$\begin{aligned} \dot{p} &= \dot{x}_1 + \dot{x}_2 \\ \Rightarrow \dot{p} &= -\omega_1 a_1 \sin(\omega_1 t + \theta_1) - \omega_2 a_2 \sin(\omega_2 t + \theta_2) \\ &= \omega_1 a_1 \cos(\omega_1 t + \theta_1 + \frac{\pi}{2}) + \omega_2 a_2 \cos(\omega_2 t + \theta_2 + \frac{\pi}{2}), \end{aligned}$$

which after adding delay effect, takes the form

$$\dot{p}_\tau = \omega_1 a_{1\tau} \cos(\omega_1 t + \theta_{1\tau} + \frac{\pi}{2} - \omega_1 \tau) + \omega_2 a_{2\tau} \cos(\omega_2 t + \theta_{2\tau} + \frac{\pi}{2} - \omega_2 \tau), (18)$$

where $a_{1\tau}$, $a_{2\tau}$, $\theta_{1\tau}$ and $\theta_{2\tau}$ are amplitudes and phases after the delay block, respectively. Since, for K-B approximation the amplitudes a_i and the phases θ_i ($i = 1, 2$) are slowly time-varying functions, and in order to approximate the time delay block, we propose the following assumption.

Assumption 1 For small time delay τ , the quantities $|a_i - a_{i\tau}|$ and $|\theta_i - \theta_{i\tau}|$ ($i = 1, 2$) can be neglected.

The assumption 1 allows the following approximations

$$\begin{cases} a_{i\tau} = a_i - (a_i - a_{i\tau}) \approx a_i, \\ \theta_{i\tau} = \theta_i - (\theta_i - \theta_{i\tau}) \approx \theta_i. \end{cases} \quad (i = 1, 2) \quad (19)$$

To get an expression in the form of (5), the low pass filter block must be also approximated. Therefore, we consider a second assumption

Assumption 2 *The low pass filter is linear and its dynamics is much faster than the evolution of amplitudes and phases.*

The utility of assumption 2 is that, for an input given as the sum of sinusoidal terms (such as (5)), the output will be equal to the sum of the outputs of each term, and for sinusoidal inputs with slowly time-varying amplitudes and phases the rise time will be neglected, and the amplitudes and phases will be considered as constant parameters. Therefore, the assumption 2 leads to the following approximation

$$LPF(a \cos(\omega t + \theta)) \approx G(\omega)a \cos(\omega t + \theta - \phi(\omega)) \quad (20)$$

where a , ω and θ are the amplitude, the frequency and the phase of input, respectively, $G(\omega)$ and $\phi(\omega)$ are the gain and the phase at frequency ω introduced by the filter. We use the following notation in the remaining of paper

$$\psi_{k_1 k_2} = (k_1 \omega_1 + k_2 \omega_2)t + (k_1 \theta_1 + k_2 \theta_2), \quad (21)$$

$$A_{k_1 k_2} = \omega_1^{|k_1|} \omega_2^{|k_2|} G(k_1 \omega_1 + k_2 \omega_2), \quad (22)$$

$$\chi_{k_1 k_2} = \frac{(k_1 + k_2)\pi}{2} - (k_1 \omega_1 + k_2 \omega_2)\tau - \phi(k_1 \omega_1 + k_2 \omega_2). \quad (23)$$

The continuation of analysis will show that this notations have important significance. Indeed, the expression (21) correspond to linear combinations of frequencies ω_1 and ω_2 present in the development of f and the expressions (22) and (23) are the gain and phase introduced by the delay plus differentiator block and filtering, respectively.

Lemma 3. *Consider the expression (18) and the assumptions 1 and 2. Then one obtains the following development*

$$\begin{aligned} f \approx & -\varphi_{v1} \left\{ \omega_1 A_{10} a_1 \left(1 - \frac{\varphi_{v3}}{\varphi_{v1}} \left(\frac{(\omega_1 a_1)^2}{4} + \frac{(\omega_2 a_2)^2}{2} \right) \right) \sin(\psi_{10} + \chi_{10}) \right. \\ & + \omega_2 A_{01} a_2 \left(1 - \frac{\varphi_{v3}}{\varphi_{v1}} \left(\frac{(\omega_2 a_2)^2}{4} + \frac{(\omega_1 a_1)^2}{2} \right) \right) \sin(\psi_{01} + \chi_{01}) \left. \right\} \\ & + \varphi_{v3} \left\{ \frac{\omega_1 A_{30} a_1^3}{4} \sin(\psi_{30} + \chi_{30}) + \frac{(2\omega_1 - \omega_2) A_{2-1} a_1^2 a_2}{4} \sin(\psi_{2-1} + \chi_{2-1}) \right. \\ & + \frac{(2\omega_1 + \omega_2) A_{21} a_1^2 a_2}{4} \sin(\psi_{21} + \chi_{21}) + \frac{(\omega_1 + 2\omega_2) A_{12} a_1 a_2^2}{4} \sin(\psi_{12} + \chi_{12}) \\ & \left. + \frac{\omega_2 A_{03} a_2^3}{4} \sin(\psi_{03} + \chi_{03}) + \frac{(2\omega_2 - \omega_1) A_{-12} a_2^2 a_1}{4} \sin(\psi_{-12} + \chi_{-12}) \right\}. \quad (24) \end{aligned}$$

Proof: substituting approximations (19) in expression (18), one gets

$$\dot{p}_\tau \approx \omega_1 a_1 \cos(\omega_1 t + \theta_1 + \frac{\pi}{2} - \omega_1 \tau) + \omega_2 a_2 \cos(\omega_2 t + \theta_2 + \frac{\pi}{2} - \omega_2 \tau). \quad (25)$$

Introducing (25), using notation (21) in nonlinear static function and trigonometrical simplifications lead to the expression

$$\begin{aligned} \varphi_{v0} + \varphi_{v1} \dot{p}_{-\tau} - \frac{\varphi_{v3}}{3} \dot{p}_{-\tau}^3 \approx \varphi_{v0} + \varphi_{v1} \omega_1 a_1 \left(1 - \frac{\varphi_{v3}}{\varphi_{v1}} \left(\frac{(\omega_1 a_1)^2}{4} + \frac{(\omega_2 a_2)^2}{2} \right) \right) \cos(\psi_{10} \\ + \frac{\pi}{2} - \omega_1 \tau) + \varphi_{v1} \omega_2 a_2 \left(1 - \frac{\varphi_{v3}}{\varphi_{v1}} \left(\frac{(\omega_2 a_2)^2}{4} + \frac{(\omega_1 a_1)^2}{2} \right) \right) \cos(\psi_{01} + \frac{\pi}{2} - \omega_2 \tau) \\ - \varphi_{v3} \left\{ \frac{(\omega_1 a_1)^3}{12} \cos(\psi_{30} + \frac{3\pi}{2} - 3\omega_1 \tau) + \frac{\omega_1^2 \omega_2 a_1^2 a_2}{4} \cos(\psi_{2-1} + \frac{\pi}{2} - (2\omega_1 - \omega_2)\tau) \right. \\ + \frac{\omega_1^2 \omega_2 a_1^2 a_2}{4} \cos(\psi_{21} + \frac{3\pi}{2} - (2\omega_1 + \omega_2)\tau) + \frac{\omega_1 \omega_2^2 a_1 a_2^2}{4} \cos(\psi_{12} + \frac{3\pi}{2} - (2\omega_2 + \omega_1)\tau) \\ \left. + \frac{(\omega_2 a_2)^3}{12} \cos(\psi_{03} + \frac{3\pi}{2} - 3\omega_2 \tau) + \frac{\omega_1 \omega_2^2 a_2^2 a_1}{4} \cos(\psi_{-12} + \frac{\pi}{2} - (2\omega_2 - \omega_1)\tau) \right\} \quad (26) \end{aligned}$$

Using (26), property (20) and notation (22), one arrives at (24).

Result (24) yields the frequency set

$$W = \{\omega_1, \omega_2, 3\omega_1, 3\omega_2, 2\omega_1 + \omega_2, \omega_1 + 2\omega_2, 2\omega_1 - \omega_2, 2\omega_2 - \omega_1\}, \quad (27)$$

which will be very important for identifying the different situations depending on the proximity of frequencies in W . Consequently, one has the following three situations:

1. $\omega_1 \not\approx \{\omega_2, 3\omega_2, \frac{\omega_2}{3}\}$,
2. $\omega_1 \approx \omega_2$: Mutual synchronization with close frequencies
3. $\omega_1 \approx 3\omega_2$ (respectively $\omega_2 \approx 3\omega_1$): Mutual synchronization with multiple frequencies

Experimental results ([11]) reveal that both modes can oscillate freely without synchronization and with the frequencies not respecting the conditions of cases number 2 and 3. Hence, we limit our study here to case 1. This is new and have clear practical implication when compared with [18].

K-B approximation of the model

The second step of analysis is to find the expression of the model outputs using the result (24) and to analyze the evolution of this outputs in different situations.

Lemma 4. *Consider the condition $\omega_1 \not\approx \{\omega_2, 3\omega_2, \frac{\omega_2}{3}\}$ and the result (24). The application of K-B approximation gives*

$$x_i = a_i \cos(\omega_i t + \theta_i), \quad (i = 1, 2) \quad (28)$$

with

$$\begin{cases} \dot{a}_1 = \frac{\varphi_{v1} A_{10} \cos(\chi_{10})}{2} a_1 \left(1 - \frac{\varphi_{v3}}{\varphi_{v1}} \left(\frac{(\omega_1 a_1)^2}{4} + \frac{(\omega_2 a_2)^2}{2} \right) \right), \\ \dot{a}_2 = \frac{\varphi_{v1} A_{01} \cos(\chi_{01})}{2} a_2 \left(1 - \frac{\varphi_{v3}}{\varphi_{v1}} \left(\frac{(\omega_2 a_2)^2}{4} + \frac{(\omega_1 a_1)^2}{2} \right) \right), \\ \dot{\theta}_1 = \frac{\varphi_{v1} A_{10} \sin(\chi_{10})}{2} \left(1 - \frac{\varphi_{v3}}{\varphi_{v1}} \left(\frac{(\omega_1 a_1)^2}{4} + \frac{(\omega_2 a_2)^2}{2} \right) \right), \\ \dot{\theta}_2 = \frac{\varphi_{v1} A_{01} \sin(\chi_{01})}{2} \left(1 - \frac{\varphi_{v3}}{\varphi_{v1}} \left(\frac{(\omega_2 a_2)^2}{4} + \frac{(\omega_1 a_1)^2}{2} \right) \right), \end{cases} \quad (29)$$

Proof: by application of rules (2) and (3) on the expression (24), one finds easily the result of K-B approximation described in lemma (4).

From the equations (29), one can see that the coupled parameters are a_1 and a_2 . Therefore, the system dynamics depend essentially on the evolution of amplitudes a_1 and a_2 . The analytical determination of equilibrium points gives

$$a_1 = 0 \text{ and } a_2 = 0, \quad (30)$$

$$a_1 = \frac{2}{\omega_1} \sqrt{\frac{\varphi_{v1}}{\varphi_{v3}}} \text{ and } a_2 = 0, \quad (31)$$

$$a_1 = 0 \text{ and } a_2 = \frac{2}{\omega_2} \sqrt{\frac{\varphi_{v1}}{\varphi_{v3}}}, \quad (32)$$

$$a_1 = \frac{2}{\omega_1} \sqrt{\frac{\varphi_{v1}}{3\varphi_{v3}}} \text{ and } a_2 = \frac{2}{\omega_2} \sqrt{\frac{\varphi_{v1}}{3\varphi_{v3}}}. \quad (33)$$

The stability of each equilibrium point leads to a particular regime. Consequently, one distinguishes four operation regimes, which will be elaborated and explained shortly :

1. Asymptotically stable system,
2. Two generators with competitive quenching,
3. Simultaneous self-sustained oscillations,
4. Total instability.

For stability study one can apply Lyapunov's indirect method, which uses the stability property of linearized system around the equilibrium point. The computation of general characteristic polynomial leads to the flowing result

$$\begin{aligned} P(\lambda) = & \lambda^2 - \frac{\varphi_{v1}}{2} \left\{ A_{10} \cos(\chi_{10}) \left(1 - \frac{\varphi_{v3}}{\varphi_{v1}} \left(\frac{3(\omega_1 a_1)^2}{4} + \frac{(\omega_2 a_2)^2}{2} \right) \right) + A_{01} \cos(\chi_{01}) \left(1 - \frac{\varphi_{v3}}{\varphi_{v1}} \left(\frac{3(\omega_2 a_2)^2}{4} + \frac{(\omega_1 a_1)^2}{2} \right) \right) \right\} \lambda \\ & + \frac{A_{10} A_{01} \cos(\chi_{10}) \cos(\chi_{01})}{4} \left\{ \varphi_{v1}^2 \left(1 - \frac{\varphi_{v3}}{\varphi_{v1}} \left(\frac{3(\omega_1 a_1)^2}{4} + \frac{(\omega_2 a_2)^2}{2} \right) \right) \left(1 - \frac{\varphi_{v3}}{\varphi_{v1}} \left(\frac{3(\omega_2 a_2)^2}{4} + \frac{(\omega_1 a_1)^2}{2} \right) \right) - \varphi_{v3}^2 (\omega_1 \omega_2 a_1 a_2)^2 \right\}. \end{aligned} \quad (34)$$

The characteristic polynomial obtained is second order. Therefore, the stability can be verified by testing the signs of polynomial coefficients.

Asymptotically stable system:

The system is asymptotically stable around the origin, if and only if the equilibrium point (30) is asymptotically stable. Introducing (30) in the general characteristic polynomial (34), one obtains

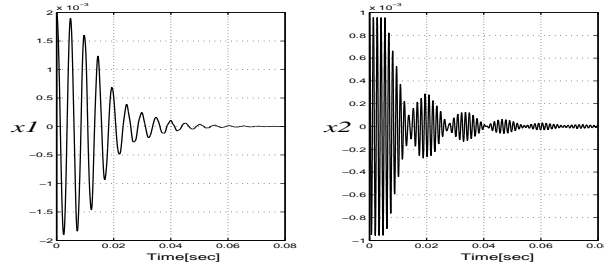


Fig. 6. Simulation test for $\omega_1 = 2\pi \times 210$, $\omega_2 = 2\pi \times 740$, $\varphi_{v0} = 0.45$, $\varphi_{v1} = -0.135$, $\varphi_{v3} = -5.4 \times 10^{-3}$, $LPF = \frac{2\pi \times 500}{s + 2\pi \times 500}$ and $\tau = 5.5 \times 10^{-3}$.

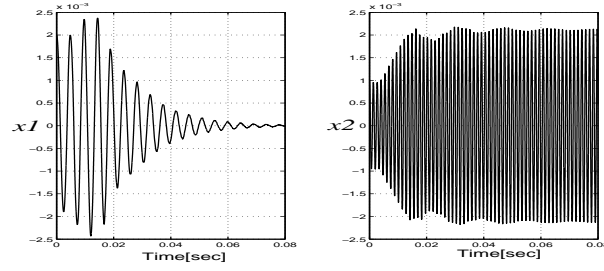


Fig. 7. Simulation test for $\omega_1 = 2\pi \times 210$, $\omega_2 = 2\pi \times 740$, $\varphi_{v0} = 0.45$, $\varphi_{v1} = -0.135$, $\varphi_{v3} = -5.4 \times 10^{-3}$, $LPF = \frac{2\pi \times 500}{s + 2\pi \times 500}$ and $\tau = 3.5 \times 10^{-3}$.

$$P(\lambda) = \lambda^2 - \frac{\varphi_{v1}}{2} \left\{ A_{10} \cos(\chi_{10}) + A_{01} \cos(\chi_{01}) \right\} \lambda + \frac{A_{10} A_{01} \cos(\chi_{10}) \cos(\chi_{01}) \varphi_{v1}^2}{4},$$

which has two stable zeros if the following conditions are respected

$$\begin{cases} -\varphi_{v1} \left\{ A_{10} \cos(\chi_{10}) + A_{01} \cos(\chi_{01}) \right\} > 0 \\ A_{10} A_{01} \cos(\chi_{10}) \cos(\chi_{01}) \varphi_{v1}^2 > 0 \end{cases} \iff \begin{cases} \varphi_{v1} \cos(\chi_{10}) < 0 \\ \varphi_{v1} \cos(\chi_{01}) < 0 \end{cases} \quad (35)$$

Provided (35) is satisfied and initial states are close to the origin, the amplitudes of both oscillations converge to equilibrium point (30). Figure 6 shows an example of simulation test, where the conditions (35) are satisfied under realistic parameters values.

Two generators with competitive quenching:

The two generators with competitive quenching regime occurs when both equilibrium points (31) and (32) are locally stable. Substituting (31) into (34), one gets

$$P(\lambda) = \lambda^2 + \varphi_{v1} \left\{ A_{10} \cos(\chi_{10}) + \frac{1}{2} A_{01} \cos(\chi_{01}) \right\} \lambda + \frac{A_{10} A_{01} \cos(\chi_{10}) \cos(\chi_{01}) \varphi_{v1}^2}{2},$$

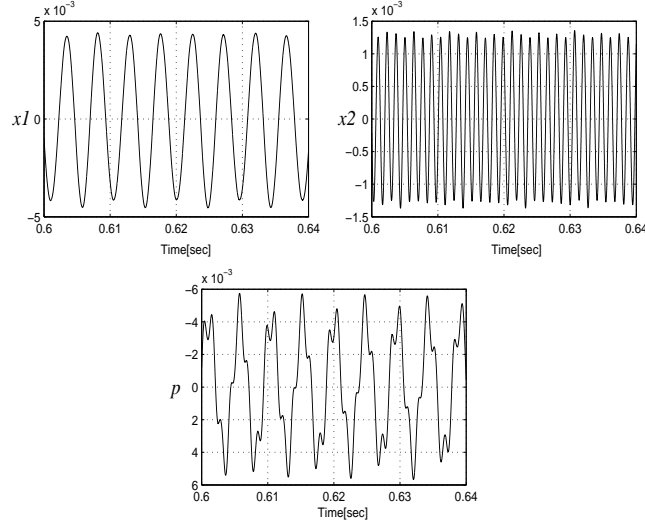


Fig. 8. Simulation test for $\omega_1 = 2\pi \times 210$, $\omega_2 = 2\pi \times 740$, $\varphi_{v0} = 0.45$, $\varphi_{v1} = -0.135$, $\varphi_{v3} = -5.4 \times 10^{-3}$, $LPF = \frac{2\pi \times 500}{s + 2\pi \times 500}$ and $\tau = 4.8 \times 10^{-3}$.

The local stability of (31) is satisfied if and only if

$$\begin{cases} \varphi_{v1} \left\{ A_{10} \cos(\chi_{10}) + \frac{1}{2} A_{01} \cos(\chi_{01}) \right\} > 0 \\ A_{10} A_{01} \cos(\chi_{10}) \cos(\chi_{01}) \varphi_{v1}^2 > 0 \end{cases} \iff \begin{cases} \varphi_{v1} \cos(\chi_{10}) > 0 \\ \varphi_{v1} \cos(\chi_{01}) > 0 \end{cases} \quad (36)$$

By symmetry, for the equilibrium point (32) one finds the same conditions.

Provided that the conditions (36) are satisfied, the amplitudes of x_1 and x_2 converge to one of both possible equilibrium points (31) and (32). Depending on the initial states, one of the generators is excited, while the oscillations of the other generator are entirely quenched. Figure 7 shows an example of simulation test on two generators with competitive quenching regime.

Simultaneous self-sustained oscillations:

Simultaneous oscillation of both resonators occurs when the equilibrium point (33) is stable. Introducing (33) in (34), one obtains

$$P(\lambda) = \lambda^2 + \frac{\varphi_{v1}}{3} \left\{ A_{10} \cos(\chi_{10}) + A_{01} \cos(\chi_{01}) \right\} \lambda - \frac{A_{10} A_{01} \cos(\chi_{10}) \cos(\chi_{01}) \varphi_{v1}^2}{3},$$

The equilibrium point (33) is locally stable if and only if

$$\begin{cases} \varphi_{v1} \left\{ A_{10} \cos(\chi_{10}) + A_{01} \cos(\chi_{01}) \right\} > 0 \\ -A_{10} A_{01} \cos(\chi_{10}) \cos(\chi_{01}) \varphi_{v1}^2 > 0 \end{cases} \iff \begin{cases} \varphi_{v1} (A_{10} \cos(\chi_{10}) + A_{01} \cos(\chi_{01})) > 0 \\ \cos(\chi_{10}) \cos(\chi_{01}) < 0 \end{cases} \quad (37)$$

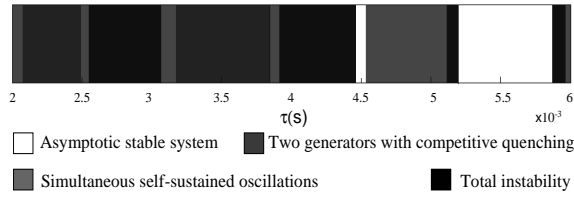


Fig. 9. The operation regimes as a function of τ , $\omega_1 = 2\pi \times 210$, $\omega_2 = 2\pi \times 740$, $\varphi_{v0} = 0.45$, $\varphi_{v1} = -0.135$, $\varphi_{v3} = -5.4 \times 10^{-3}$ and $LPF = \frac{2\pi \times 500}{s + 2\pi \times 500}$.

By satisfying (37), it is possible to have simultaneous self-sustained oscillations, the amplitudes of x_1 and x_2 converge to the equilibrium point (33). By the self-sustained oscillations it is meant that both oscillators are excited without synchronization. The Figure 8 shows the stationary part of a simulation test example on simultaneous self-sustained oscillations regime.

Total instability:

When the conditions (35), (36) and (37) are not satisfied, there does not exist a stable equilibrium point. Therefore, there is no stable limit cycle and the amplitudes of both oscillations diverge. By total instability it is meant that for any initial states, the oscillations of the system diverge.

Results analysis

The results demonstrate the existence of four operation regimes when the ratio of natural frequencies is different from 1, 3 and $\frac{1}{3}$. The occurrence of each operation regime depends on the satisfaction of some conditions. The simulations confirm the quality of estimated amplitudes using K-B approximation. The condition for each regime contain essentially the phases χ_{01} and χ_{10} introduced by the delay and low pass filtering respectively. The phase domain conditions (35), (36) and (37) are independent. So with fixed delay and low-pass filter it is not possible to have operation in more than one regime. The results suggest that it is perhaps possible in certain cases to estimate the delay from the measurement of the oscillations (number, frequency, amplitude). To illustrate the importance of delay, Figure 9 depicts the operation regimes for several values of τ and for other parameters fixed near to the practical values. One observes the occurrence of various regimes as a function of the delay.

From a practical point of view, the interesting situation is the simultaneous self-sustained oscillatory regime which is represented in Figure 9. The fact that, the amplitudes of harmonics ω_1 and ω_2 take values $\frac{2}{\omega_1} \sqrt{\frac{\varphi_{v1}}{3\varphi_{v3}}}$ and $\frac{2}{\omega_2} \sqrt{\frac{\varphi_{v1}}{3\varphi_{v3}}}$ respectively, shows clearly that they depend inversely on the values of frequencies (phenomenon which has been observed in practice). The results

of Figure 9 have a very important practical implication : the design of the combustion system influence the type of combustion instability which may occurs.

5 Quenching of the oscillations

For the development of effective control method for quenching both oscillation modes present in combustion instabilities, the model (15) is taken by adding a multiplicative control action (modulation of the fuel flow). The multiplicative effect of the control action must be included in the representation to capture the modulation of a fraction of the fuel flow u into the combustion chamber and its consequent effect on the heat release rate [11, 10]. This leads to the following differential equations.

$$\begin{cases} \ddot{x}_1 + \omega_1^2 x_1 = \frac{d}{dt} LPF \left\{ (1+u) \left(\varphi_{v0} + \varphi_{v1} \dot{p}_\tau - \frac{\varphi_{v3}}{3} \dot{p}_\tau^3 \right) \right\}, \\ \ddot{x}_2 + \omega_2^2 x_2 = \frac{d}{dt} LPF \left\{ (1+u) \left(\varphi_{v0} + \varphi_{v1} \dot{p}_\tau - \frac{\varphi_{v3}}{3} \dot{p}_\tau^3 \right) \right\}. \end{cases} \quad (38)$$

To deal with combustion instabilities, different approaches are considered in practice [5]. One can use a feedback control which is based on using the pressure measurement. Two types of control law can be considered, one linear the other nonlinear. The linear law need the availability of x_1 and x_2 which can be obtained by using appropriate band pass filters [20]. Here we are interested on the non-linear feedback which use the pressure measurement ($p = x_1 + x_2$), since it gives effective results and is subject to less constrains. To study the effects of such control we use the K-B method. The following assumption is proposed concerning the validity of the K-B approximation.

Assumption 3 *Let a_1 and a_2 be the amplitudes of the oscillations x_1 and x_2 obtained from K-B approximation. If a_1 and a_2 are asymptotically locally (globally) stable at the origin, then the original system is asymptotically locally stable at the origin.*

For non-linear feedback, the pressure measurement p is differentiated and delayed with a delay τ to obtain \dot{p}_τ , which is introduced into a non-linear function Φ , to obtain a control law $u = \Phi(p, \dot{p}_\tau)$. This control strategy is explained in the block diagram shown in Figure 10. This control law will be used to add damping and to compensate the physical feedback caused by the coupling between the thermal heat-release process and the acoustics of the combustion chamber. If such a control is designed, the system will be asymptotically stable at the origin and the quenching of oscillations will occur. This can be interpreted also as a feedback linearization which in addition stabilizes the system. The results are summarize in the following lemma

Lemma 5. *For the control law*

$$\Phi(p, \dot{p}_\tau) = -Kp - \frac{1}{\varphi_{v0}} \left(\varphi_{v1} \dot{p}_\tau - \frac{\varphi_{v3}}{3} \dot{p}_\tau^3 \right), \quad (39)$$

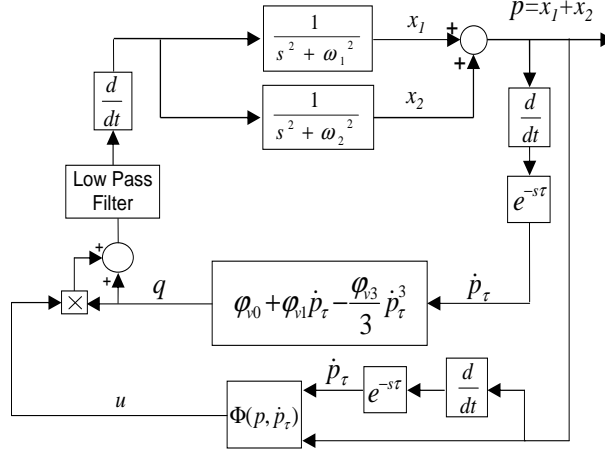


Fig. 10. Block diagram of non-linear feedback.

where K is a constant satisfying the conditions

$$\begin{cases} K\varphi_{v0} \cos(\phi(\omega_1)) > 0, \\ K\varphi_{v0} \cos(\phi(\omega_2)) > 0, \end{cases} \quad (40)$$

the system is locally asymptotically stable at the origin.

Proof: Replacing the function (39) in (38) yields,

$$\begin{cases} \ddot{x}_1 + \omega_1^2 x_1 = \frac{d}{dt} LPF \left\{ \varphi_{v0} - K\varphi_{v0}p - K\varphi_{v1}p\dot{p}_\tau + K\frac{\varphi_{v3}}{3}p\dot{p}_\tau^3 \right. \\ \quad \left. - \frac{\varphi_{v1}^2}{\varphi_{v0}}\dot{p}_\tau^2 + \frac{2\varphi_{v1}\varphi_{v3}}{3\varphi_{v0}}\dot{p}_\tau^4 - \frac{\varphi_{v3}^2}{9\varphi_{v0}}\dot{p}_\tau^6 \right\}, \\ \ddot{x}_2 + \omega_2^2 x_2 = \frac{d}{dt} LPF \left\{ \varphi_{v0} - K\varphi_{v0}p - K\varphi_{v1}p\dot{p}_\tau + K\frac{\varphi_{v3}}{3}p\dot{p}_\tau^3 \right. \\ \quad \left. - \frac{\varphi_{v1}^2}{\varphi_{v0}}\dot{p}_\tau^2 + \frac{2\varphi_{v1}\varphi_{v3}}{3\varphi_{v0}}\dot{p}_\tau^4 - \frac{\varphi_{v3}^2}{9\varphi_{v0}}\dot{p}_\tau^6 \right\}. \end{cases}$$

Therefore, for the K-B approximation (1) with $\epsilon = 1$ one may consider the following choice.

$$f_1 = f_2 = f = \frac{d}{dt} LPF \left\{ \varphi_{v0} - K\varphi_{v0}p - K\varphi_{v1}p\dot{p}_\tau + K\frac{\varphi_{v3}}{3}p\dot{p}_\tau^3 \right. \\ \quad \left. - \frac{\varphi_{v1}^2}{\varphi_{v0}}\dot{p}_\tau^2 + \frac{2\varphi_{v1}\varphi_{v3}}{3\varphi_{v0}}\dot{p}_\tau^4 - \frac{\varphi_{v3}^2}{9\varphi_{v0}}\dot{p}_\tau^6 \right\}. \quad (41)$$

Introducing $x_i = a_i \cos(\omega_i t + \theta_i)$ and $\dot{x}_i = -a_i \omega_i \sin(\omega_i t + \theta_i)$, $i = 1, 2$, in (41), using the approximation (25) and after trigonometric simplifications and using assumption 2, one obtains the expression

$$f \approx K\varphi_{v0}\omega_1 G(\omega_1)a_1 \left[\cos(\phi(\omega_1)) \sin(\omega_1 t + \theta_1) - \sin(\phi(\omega_1)) \cos(\omega_1 t + \theta_1) \right] \\ + K\varphi_{v0}\omega_2 G(\omega_2)a_2 \left[\cos(\phi(\omega_2)) \sin(\omega_2 t + \theta_2) - \sin(\phi(\omega_2)) \cos(\omega_2 t + \theta_2) \right] \\ + \sum_{\omega_\ell \neq \omega_1 \wedge \omega_2}^r (H_\ell(a_1, a_2, \theta_1, \theta_2) \sin(\omega_\ell t + \theta_\ell) + G_\ell(a_1, a_2, \theta_1, \theta_2) \cos(\omega_\ell t + \theta_\ell)).$$

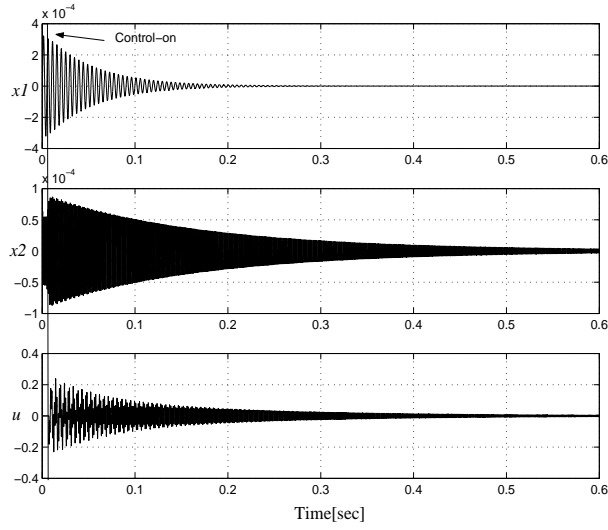


Fig. 11. Linear feedback control applied at the first appearance of oscillations.

Applying the rule (3) for the amplitudes leads to the following approximations.

$$\begin{cases} \frac{da_1}{dt} = -\frac{1}{2}G(\omega_1)K\varphi_{v0} \cos(\phi(\omega_1))a_1, \\ \frac{da_2}{dt} = -\frac{1}{2}G(\omega_2)K\varphi_{v0} \cos(\phi(\omega_2))a_2. \end{cases} \quad (42)$$

These are linear differential equations for the uncoupled amplitudes a_1 and a_2 . The amplitudes are globally asymptotically stable at origin if the conditions (40) are satisfied. Appealing to the assumption 3, one deduces the result.

This control has been tested in simulation, with the same model parameters used in simultaneous self-sustained oscillations and with gain $K = 100$ for the two possible scenarios. In the first scenario, the control is applied at the appearance of oscillations in x_1 or x_2 . This is presented in Figure 11. In the second scenario, the control is applied after that the oscillations of x_1 and x_2 have already reached steady-state operation. This is presented in Figure 12.

The control law yields asymptotic local stability at the origin. The domain of amplitudes a_1 and a_2 where quenching oscillations is guaranteed, is delimited by the boundary of validity the K-B method applied to (38). It is important to note however, that such control strategy requires good knowledge of the parameters values in the combustion instability model, particularly of the value of the delay τ .

6 Conclusion

This paper presents a model for combustion instabilities which is analytically tractable. Its analysis is carried on using the Krylov - Bogoliubov(K-B)

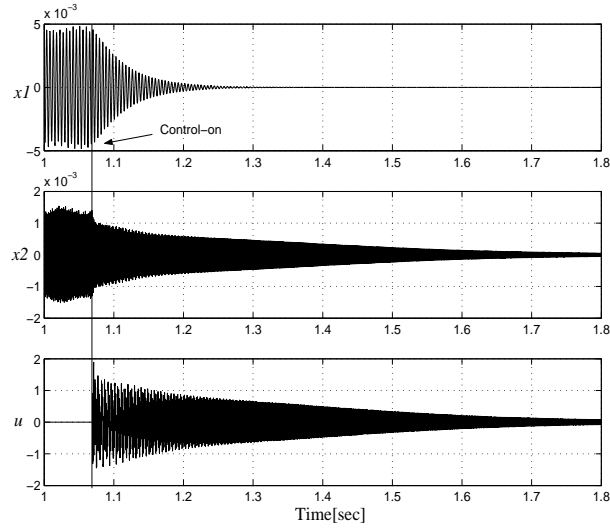


Fig. 12. Non-linear feedback control applied after the oscillation has reached steady-state.

method. The analysis has shown that the model can explain the coexistence of several distinct non-harmonic frequencies observed in practice. The paper has also shown and quantified the effect of the delay for the occurrence of the various phenomena observed.

Once that a method of analysis has been made available and taking advantage of the multiplicative control which can be implemented by amplitude modulation of the fuel flow, a feedback control methodology for quenching oscillations in combustion instabilities has been developed. The possibility of quenching oscillations has been analyzed also by the K-B method.

Further work will focus on robustness of these quenching approaches with respect to model parameters uncertainties as well as a quantitative evaluation of the stability domains.

References

1. J. Tyndal, *Sound*. New York: D. Appleton & Company, 1897.
2. K. McManus, F. Han, W. Dunstan, C. Barbu, and M. Shah, "Modeling and control of combustion dynamics in industrial gas turbines," *Proc. ASME Turbo-Expo*, pp. 567–575, 2004.
3. E. H. M. Mettenleiter and S. Candel, "Adaptive control of aeroacoustic instabilities," *J. Sound & Vibration*, vol. 230, no. 4, pp. 761–789, 2000.
4. A. Dowling, "The calculation of thermoacoustic oscillations," *J Sound & Vibration*, vol. 180, no. 4, pp. 557–581, 1995.

5. A. Annaswamy and A. Ghoniem, "Active control of combustion instability: Theory and practice," *IEEE Control Systems Magazine*, vol. 22, no. 6, pp. 37–54, Dec 2002.
6. P. Rijke, *Ann. of Physics*, 1959.
7. G. Roy, *Advances in Chemical Propulsion: Science to Technology*. Boca Raton, FL USA: CRC – Taylor & Francis, 2001.
8. A. Banaszuk, K. Ariyur, M. Krstic, and C. Jacobson, "An adaptive algorithm for control of combustion instability," *Automatica*, vol. 40, pp. 2155–2162, 2004.
9. R. M. Murray, C. A. Jacobson, R. Casas, A. I. Khibnik, C. R. Johnson Jr, R. R. Bitmead, A. A. Peracchio, and W. M. Proscia, "System identification for limit cycling systems: a case study for combustion instabilities," *American Control Conference, Philadelphia PA*, pp. 2004–2008, 1998.
10. W. J. Dunstan, R. R. Bitmead, and S. M. Savaresi, "Fitting nonlinear low-order models for combustion instability control," *Control Engineering Practice*, pp. 1301–1317, 2001.
11. W. J. Dunstan, "System identification of nonlinear resonant systems," Ph.D. dissertation, University of California, San Diego, 2003.
12. N. Bogoliubov and Y. Mitropolski, *Asymptotic Methods in the Theory of Nonlinear Oscillations*. New York: Hindustan Publishing Corp, Delhi, and Gordon and Breach, 1961.
13. C. Hayashi, *Nonlinear Oscillations in Physical Systems*. New York: McGraw-Hill Book Co, 1964, (reprinted by Princeton University Press, 1985).
14. P. S. Landa, *Nonlinear Oscillations and Waves in Dynamical Systems*. Kluwer, 1996.
15. —, *Regular and Chaotic Oscillations*. New York: Springer, 2000.
16. I. D. Landau and R. R. Bitmead, "On the method of Krylov and Bogoliubov for the analysis of nonlinear oscillations," Mechanical and Aerospace Engineering Department, University of California, San Diego, 9500 Gilman Drive, La Jolla CA 92093-0411, USA, Tech. Rep., Jan 2004.
17. H. K. Khalil, *Nonlinear Systems*. New York: MacMillan, 1992.
18. F. Bouziani, I. D. Landau, R. R. Bitmead, and A. Voda-Besançon, "An analytically tractable model for combustion instability," *IEEE Conference on Decision and Control and European Control Conference, Sevilla*, 2005.
19. —, "Analysis of a tractable model for combustion instability: the effect of delay and low pass filtering," *Conference on Decision and Control, San Diego*, 2006.
20. F. Bouziani, I. D. Landau, and R. R. Bitmead, "Quenching oscillations in combustion instabilities using model-based closed-loop multiplicative control," Laboratoire d'Automatique de Grenoble, ENSIEG BP 46, 38402 Saint-Martin d'Hères, France, Tech. Rep., November 2006.